

Quasar outflows and the formation of dwarf galaxies

Priyamvada Natarajan¹, Steinn Sigurdsson¹ and Joseph Silk^{1,2,3}

1. Institute of Astronomy, Madingley Road, Cambridge CB3 0HA, U. K.
2. Department of Astronomy and Physics, Univ. of California at Berkeley, Berkeley, CA 97420, U. S. A.
3. Center for Particle Astrophysics, Univ. of California at Berkeley, Berkeley, CA 97420, U. S. A.

Received —; accepted —

ABSTRACT

We propose a scenario for the formation of a population of baryon-rich, dark matter-deficient dwarf galaxies at high redshift that form from the mass swept out in the Intergalactic Medium (IGM) by energetic outflows from luminous quasars. We predict the intrinsic properties of these galaxies, and examine the prospects for their observational detection in the optical, X-ray and radio wavebands. Detectable thermal Sunyaev-Zeldovich decrements (cold spots) on arc-minute scales in the cosmic microwave background radiation maps are expected during the shock-heated expanding phase from these hot bubbles. We conclude that the optimal detection strategy for these dwarfs is via narrow-band Lyman- α imaging of regions around high redshift quasars. An energetically scaled-down version of the same model is speculated upon as a possible mechanism for forming pre-galactic globular clusters.

Subject headings: cosmology: observations – cosmology: gravitational lensing – clusters – galaxies: clusters

1. Introduction

Galaxy formation is a complex physical process involving several length, mass and time scales, and it is therefore expected to proceed in a fashion that is modulated by the properties of the local environment in which it occurs. In the context of a hierarchical picture for structure formation in a cold dark-matter dominated Universe, most massive galaxies are thought to assemble fairly recently (at $z \sim 0.5 - 1$) from the agglomeration of sub-clumps that have collapsed at higher redshifts (White & Frenk 1991; Kauffmann, White & Guiderdoni 1993; Baugh et al. 1997). Recent observations from the Hubble Space Telescope (*HST*) and ground-based telescopes find that a significant fraction of the stellar mass as traced by blue light, and that constitute galaxies, is in place by redshift $\sim 1.5 - 2.0$ (Madau 1996; Lilly et al. 1996). The other cosmological objects in place by these redshifts are quasars; and given the high bolometric luminosities of high redshift quasars it is natural to expect that they probably play an important role in locally modulating galaxy formation (Efstathiou & Rees 1988; Babul & White 1991; Babul & Rees 1992).

We propose that quasars effect galaxy formation in their vicinity via energetic outflows. The outflow powered by the mechanical luminosity of the quasar shocks and sweeps out mass from the IGM into a (thin) shell that propagates out on scales of the order of a few hundred kpc or so. The swept-up matter expands adiabatically till a gravitational instability of the shell causes it to fragment, yielding clumps with a typical mass-scale, $\sim 10^9 M_{\odot}$ corresponding to the mass of dwarf galaxy-size objects, akin to the explosion-driven galaxy formation scenarios proposed by Mckee & Ostriker (1977), Ostriker & Cowie (1981) and Ostriker & Ikeuchi (1983). The propagation of these cosmological blast-waves has been computed by Ostriker & Cowie (1981), Bertschinger (1985), Vishniac, Ostriker & Bertschinger (1985), Carr & Ikeuchi (1985), Tegmark, Silk & Evrard (1993) in slightly different contexts, that of explosion-induced structure formation models or the role of supernovae winds. In recent papers, Voit (1994; 1996) has examined the effects of quasar-blown bubbles on the structure of the Inter-Galactic Medium. Here we focus on the fate of the gas in these bubbles. We consider the basic scaling relations for our proposed model in the second section of this paper. In Section 3, we outline the dynamics of quasar outflows and the fate of the cold dense gas deposited in shells around the quasar, when gravitational instability causes mass clumps to form on the scale of dwarf galaxies. In Section 4, the predicted properties and prospects for detection of this population of dwarfs and the outflow in the optical and X-ray wave-bands are explored. We then note that the high-redshift blue clumps detected by *HST* reported by Pascarelle et al. (1996) and the galaxies detected in the Lyman- α by Hu & McMahon (1996) are potential candidates (Section 5). Before concluding, we speculate on the consequences of a scaled-down version of the same scenario for the formation of the pre-galactic globular cluster population.

2. Quasar outflows

The total energy budget available from a quasar to power the mechanical luminosity of the outflow is determined by the mass accreted by a black hole of mass M_{bh} modulo two efficiency factors: one that determines the conversion of rest mass into the bolometric luminosity ϵ (~ 0.1), and the efficiency of conversion of the bolometric luminosity into mechanical luminosity parameterized as ϵ_L (~ 0.5). Bolometric luminosities of bright quasars at redshifts $z \gtrsim 2$ are as high as $\sim 10^{47} \text{ erg s}^{-1}$ or larger. A typical outflow can therefore sweep up mass M_{IGM} from the IGM:

$$M_{\text{IGM}} \sim 2 \times 10^{12} \left(\frac{L_{\text{QSO}}}{10^{47} \text{ erg s}^{-1}} \right) \left(\frac{\delta t}{5 \times 10^7 \text{ yr}} \right) \times \left(\frac{v_{\text{flow}}}{3000 \text{ km s}^{-1}} \right)^{-2} M_{\odot}, \quad (1)$$

where δt is the duration of the wind phase/the lifetime of the quasar, v_{flow} the outflow velocity and L_{QSO} the mechanical luminosity of the quasar. The outflow extends to:

$$R \sim 500 \left(\frac{\epsilon \epsilon_L}{0.05} \right)^{1/3} \left(\frac{M_{\text{bh}}}{10^9 M_{\odot}} \right)^{1/3} \left(\frac{f_Q}{0.01} \right)^{-1/3} \times \left(\frac{v_{\text{flow}}/c}{0.01} \right)^{-2/3} \text{ kpc}. \quad (2)$$

where f_Q is the local baryon fraction in units of 0.01. Note that if the density of the ambient medium is lower, then the outflow expands out to larger scales. All the numbers quoted in this work have been computed for $H_0 = 50 \text{ km s}^{-1} \text{ Mpc}$; $\Omega_0 = 1.0$ and $\Lambda = 0$.

3. Outflow dynamics

Below, we summarize the dynamical sequence before estimating the relevant numbers. In this treatment, we ignore the detailed microphysics of the outflow from the BH, but assume that the flow is a mildly relativistic and directed one involving only a small mass at the base of the outflow. We also ignore the time evolution of the initial stages of the outflow and consider the dynamics of the outflow only at the epoch when the swept-up mass is comparable to or greater than the mass of the BH M_{bh} .

During the lifetime of the quasar ($t_Q \sim 5 \times 10^7 \text{ yr}$), the outflow expands freely into the IGM, shock-heating material locally to high temperatures $\sim 10^8 \text{ K}$. During the hot phase, we expect X-ray emission from the shocked material. For quasars that switch on at high redshifts ($z > 7$) inverse Compton cooling will dominate but at lower redshifts, the shocks expand adiabatically and cool radiatively. As the mass accumulated around the shock becomes dynamically significant, a reverse shock propagates, thermalizing the gas that is concentrated along a thin shell. This shell subsequently evolves adiabatically,

akin to supernova remnants until the age of the bubble becomes comparable to the total elapsed Hubble time at that redshift, at which juncture cosmological effects alter the structure of the outflow and its growth.

Outflows originating after $z \sim 7$, with energies greater than 10^{57} erg remain adiabatic to low redshifts (Bertschinger 1985). The assumption of adiabatic expansion remains valid (the post-shock density being roughly four times the density of the ambient IGM; and the radius $R(t)$ of the bubble scaling as $t^{2/5}$ once the QSO shuts off) until the shell of mass swept-up at the shock front becomes self-gravitating. In this treatment we focus on the dynamics of the outflows during this radiative cooling dominated stage. They are well-approximated by the family of self-similar Sedov-Taylor blast-wave solutions (McKee & Ostriker 1977; Bertschinger 1985; Voit 1994; Voit 1996) at this epoch. The swept-up mass becomes dynamically important at a time t after the commencement of the outflow:

$$t \sim 5 \times 10^7 (1+z)^{-3/2} \Omega_{\text{IGM}}^{-1/2} \left(\frac{\dot{M}}{4 \times 10^4 M_{\odot} \text{ yr}^{-1}} \right)^{1/2} \times \left(\frac{v_{\text{flow}}}{3000 \text{ kms}^{-1}} \right)^{-1/2} \text{ yr}, \quad (3)$$

where \dot{M} is the mean outflow rate (i.e. $M_{\text{IGM}}/t_{\text{Q}}$) in units of $4 \times 10^4 M_{\odot} \text{ yr}^{-1}$ and Ω_{IGM} is the mass density of the IGM (where $\Omega_{\text{IGM}} \ll \Omega_0$), at which time the bubble radius is:

$$R \sim 400 (1+z)^{-3/2} \Omega_{\text{IGM}}^{-1/2} \left(\frac{\dot{M}}{4 \times 10^4 M_{\odot} \text{ yr}^{-1}} \right)^{1/2} \times \left(\frac{v_{\text{flow}}}{3000 \text{ kms}^{-1}} \right)^{-1/2} \text{ kpc}. \quad (4)$$

Eventually, as the age of the bubble approaches the local Hubble time, the cold shell of accumulated material fragments due to gravitational instability (although in principle, while Rayleigh-Taylor instabilities could set in, they do not result in the formation of gravitationally bound fragments). The boundary conditions immediately prior to fragmentation can be estimated following the treatment of Ostriker & Cowie (1981) and Voit (1994). The radiative cooling time τ_{cool} is:

$$\tau_{\text{cool}} = 1.2 \times 10^8 \left(\frac{T}{10^5 \text{ K}} \right)^{11/5} (1+z)^{-3} \text{ yr}. \quad (5)$$

Equating the radiative cooling time to the age of the bubble, an expression for the post-shock velocity v_{cool} can be obtained (Ostriker & Cowie 1981) in terms of the total energy injected into the outflow,

$$v_{\text{cool}} \sim 150 \left(\frac{L_{\text{QSO}}}{10^{47} \text{ ergs}^{-1}} \right)^{1/20} \left(\frac{\delta t}{5 \times 10^7 \text{ yr}} \right)^{1/20} (1+z)^{1/3} \text{ km s}^{-1}. \quad (6)$$

The shell temperature can be related to the total sweep-up mass as follows,

$$T_{\text{shell}} = 1.4 \times 10^5 \left(\frac{M_{\text{sweep}}}{10^{12} M_{\odot}} \right)^{2/5} (1+z)^{3/5} \text{ K} \quad (7)$$

The maximum mass that can cool during the radiative cooling phase is $10^{12} M_{\odot}$ and fragments less than $10^9 M_{\odot}$ are not Jeans unstable at this epoch, thereby naturally providing typical mass scales. Fragmentation on a scale ξ can therefore occur if a small disk of radius ξ and mass $\sim M_{\text{sweep}} \xi^2 / R^2$ extracted from the shell has a gravitational collapse time that is less than the sound-crossing time along 2ξ . The instability therefore imprints a characteristic mass scale,

$$M_{\text{frag}} \sim 5 \times 10^9 \left(\frac{E}{10^{63} \text{ erg}} \right)^{-3/10} (1+z)^{1/5} M_{\odot}, \quad (8)$$

which is roughly $10^{9-10} M_{\odot}$ (McKee & Ostriker 1977; Ostriker & Cowie 1981) for the numbers in equations (1) and (2); leading to the formation of a group of dwarf galaxies around the quasar from the total swept-up mass. While these clumps are not generally bound to each other, they are highly clustered both spatially and in velocity space. Note here that lower energy outflows imply a high fragment mass although a smaller value of the gas mass is swept up initially. Therefore weaker outflows from lower luminosity QSOs or super-winds (Barthel & Miley 1988; Heckman, Armus & Miley 1987) could be important for the formation of dark matter-poor galaxies at lower redshifts.

The final fate of the post-fragmentation outflow material, whether it is likely to stall and fall back, coast to infinity (in practice effectively till it matches on to the Hubble flow), or if it does escape the central potential well but remains bound initially on radial orbits to the proto-cluster assembling around the quasar, depends both on the energy output of the quasar and on the depth of the local potential (i. e. if the quasar is indeed at the bottom of a putative cluster potential well) and on the amount of matter the outflow runs into before it reaches low density regions and matches on to the Hubble flow. For a given density profile of dark matter around the quasar, the fragments either stall and fall back onto the quasar or continue to expand freely till they match on to the Hubble flow. The condition for fall-back can be estimated using a density profile $\rho(r)_{\text{DM}}$ to describe the dark matter profile around the quasar. The fragments coast on only if v_{flow} exceeds the local escape velocity v_{esc} of the total potential at a given distance r from the nucleus:

$$v_{\text{esc}} \sim 3000 \left(\frac{M(r)}{10^{15} M_{\odot}} \right)^{1/2} \left(\frac{r}{1 \text{ Mpc}} \right)^{-1/2} \text{ km s}^{-1} \quad (9)$$

3.1. Traditional scenarios for the formation of dwarfs

Dwarf galaxies can form directly from the collapse of cosmological density fluctuations at high redshift (Ikeuchi & Norman 1987), in which case we expect them to be dark matter-dominated. This is especially likely since the first generation of star formation may unbind most of the gas in the disk (Dekel & Silk 1986), unless the disk formed from a high angular momentum perturbation and has low surface density with sparse star formation, in which case we would see the high z counter-part of a gas rich object with a

dark matter-dominated rotation curve at low z (de Blok, McGaugh & van der Hulst 1996).

Babul & Rees (1992), however, have argued that the cosmological collapse of dwarf galaxy-scale masses is inhibited until $z \leq 1$ due to the photo-ionization of the IGM by the metagalactic UV radiation. Therefore, their model and subsequent work by Babul & Ferguson (1996) predict a formation scenario for low-mass galaxies at recent epochs that fade after a burst of star formation at $0.5 \leq z \leq 1$. These resultant low luminosity, low surface brightness objects are claimed to dominate the blue number counts at faint magnitudes in redshift surveys (Ellis 1997).

Interactions of large, gas-rich spirals may also lead to the formation of gas-rich, dark matter-poor dwarf galaxies by the fragmentation of extended or unbound tidal tails (Dubinski, Mihos & Hernquist 1996). Such dwarfs would form in small numbers near major mergers and are likely to fade rapidly after the initial burst of star formation, and would only be seen in the close vicinity of recently merged spirals.

The population of dwarf galaxies postulated here is distinguished by forming predominantly at high redshift, in large groups spread in an approximate sheet-like geometry over \sim Mpc scales. These dark matter-deficient objects (in contrast with the dark-matter dominant local dwarf galaxy population) are characterized by low amplitude rotation curves and low central velocity dispersions. Since they form from the fragmentation of a thin shell, the clumps have low specific angular momentum and are hence likely to collapse into relatively compact structures, with a brief star forming phase until supernovae remove or disperse the bulk of the remaining gas (Dekel & Rees 1986; Couchman & Rees 1986).

4. Predicted properties of the population

The dwarf galaxies that form from the cooling of these fragments are expected to have the following properties:

- they are baryon-rich and dark matter-deficient, and so the typical rotation curve will have a much lower amplitude than, say, for a local dwarf with a comparable luminous mass;
- hence these dwarf galaxies are expected to have disk-dominated rotation curves.
- Since the swept-up material is principally from the IGM at high redshift and is not very enriched, the dwarfs are expected to be metal-poor, with $\langle Z \rangle \sim 10^{-2} Z_{\odot}$,
- since they do not contain significant amounts of dark matter, we expect that the first few supernovae (SN) can entirely disrupt the remaining gas disk, truncating star formation, and therefore the surface

number density of these galaxies per square degree is likely to decline rapidly at lower redshifts, as the galaxies fade after the initial burst of star formation.

- These dwarfs are expected to be highly clustered as they form in a sheet around the quasar. Therefore, any line of sight to a background quasar through a group of nascent dwarfs, may intersect many individual members with narrow velocity spacing, producing a characteristic signature in the absorption line profiles. Each absorption line would also be relatively narrow compared to lines of the same column density at low redshifts, as the internal velocity dispersion of these dark matter deficient galaxies is lower, and since the associated gravitational potentials are fairly shallow, while their baryonic fraction is extremely high.
- the gas that settles down into the disk in these systems is likely to form compact, sub-critical disks (sub- L_*) and hence star-formation is likely to ensue in intense bursts, in isolated knots,
- since they form from gas clumps with low specific angular momentum, the gas can be funnelled in to the center very efficiently to form a compact central object. Therefore, these dwarfs are likely to harbor weak AGN, with narrow-emission lines - $M_{BH} \lesssim 10^6 M_\odot$, with luminosities less than 10^{44} erg/s.
- Given the typical gas masses of these dwarfs, using a standard Schmidt law for the conversion of gas into stars we estimate star formation rates of the order of 30 - 60 $M_\odot \text{ yr}^{-1}$.
- If these dwarfs/pre-fragmentation gas clumps remain weakly bound to the proto-cluster potential, they may form stars and avoid falling back to the central galaxy if strong inhomogeneities in the potential scatter them onto tangential orbits in the proto-cluster. In such cases, it is conceivable that a trace of this population might be observable even in the local neighbourhood, despite the fact that the tidal forces in the cluster would likely have disrupted the dwarf galaxies themselves. With $\sim 10^{10}$ stars per dwarf, we might expect a few bright planetary nebulae (PN) per (disrupted) dwarf galaxy. These PN would contribute to the apparent extra-galactic background of PN detected in local clusters (Ciardullo et al. 1997; Ferguson et al. 1997; Ciardullo, Jacoby & Ford 1989). These PN would be distinguishable via their clumpy, locally flat density distribution, with small velocity separation, since we expect the internal dispersion of the dwarfs to be small. Even after disruption, the stars and hence PN tracers of the stellar population would stay as moving groups, shearing out only over several cluster dynamical times. It is possible that deep imaging would reveal an excess of fainter PN near individual bright PN, thereby, tracing the stellar populations of the dwarf clumps of stars.

- these dwarfs are expected to be detected in the radio, via their low-level emission from the weak central AGN; in the optical, as a consequence of a burst of star-formation; via being significantly magnified as a result of gravitational lensing; or via narrow-band Lyman- α imaging by detecting either the presence of the warm, diffuse gas or emission from the dwarfs undergoing their first episode of star-formation.

Despite the fact that the covering fraction of these systems along the line of sight to a background QSO is small, they might well be detectable, being gas rich, in absorption, perhaps explaining the curious fact that the Lyman-limit systems detected by Steidel et al. (1996; 1997) using the color selection criteria at high redshift ($z \geq 3$) are **not** the optical counter-parts of the absorbers seen in quasar spectra in the same redshift range (unlike the case at low redshifts where such a correspondence has been well-established). This latter observation suggests that the absorption at high-redshifts is probably being produced by gas-rich galaxies similar to these dwarfs that are either yet to commence their first episode of star formation or are intrinsically very faint.

4.1. X-ray emission predictions

In the following calculation of the X-ray emission, we assume that a virialized cluster has **not** assembled around the quasar although the quasar might seed an over-dense region. Therefore any associated X-ray emission arises primarily due to shock-heating of the outflow. During the early adiabatic expansion phase of the hot, shocked layer of the bubble, high temperatures are expected $\sim 10^8$ K. Therefore, prior to cooling, we expect to see X-ray emission from the hot bubble. We model the density profile of the hot bubble with a constant density out to radius $(R - w)$, where $R \sim 1$ Mpc and w the width of the shell. Using the standard Hugoniot jump conditions across a strong shock, the shell density at the outer edge is four times the central value;

$$n_e(r) = n_0 \quad 0 \leq r \leq (R - w); \quad (10)$$

$$n_e(r) = 4n_0 \quad (R - w) \leq r \leq R. \quad (11)$$

Outside R , the density is assumed to be that of the ambient IGM. This profile shape is motivated by the density profile found by Bertschinger (1985) for the adiabatic cosmological detonation wave propagation solution. The thickness w is estimated to be, $w \sim t_{\text{cool}} v_{\text{shock}} \sim 100$ kpc. The central density n_0 is computed by requiring that the enclosed mass within radius R is equal to the total mass ($M_{\text{flow}} \sim 10^{12} M_{\odot}$) swept up by the outflow, which gives $n_0 \sim 10^{-2} \text{ cm}^{-3}$. The total emissivity is given by:

$$\epsilon(r) = 1.4 \times 10^{-27} T_e^{\frac{1}{2}} n_e^2(r) \text{ erg s}^{-1} \text{ cm}^{-3}; \quad (12)$$

and the integrated bolometric X-ray luminosity,

$$L_X = \int_0^{r_{\max}} \epsilon(r) 4\pi r^2 g(\theta_{\text{open}}) dr \quad \text{erg s}^{-1} \quad (13)$$

where $g(\theta_{\text{open}})$ takes into account the opening angle of the outflow. The total X-ray flux from a bubble at redshift z can then be easily computed to examine the feasibility of detection. In Fig. 1, we plot the allowed region for given physical properties (central gas density n_0 and temperature for a significant detection (5σ) by ROSAT, ASCA and AXAF at their flux detection limits, respectively, 10^{-14} erg cm $^{-2}$ s $^{-1}$, $10^{-15.5}$ erg cm $^{-2}$ s $^{-1}$ and 10^{-15} erg cm $^{-2}$ s $^{-1}$; during a 10^3 ks integration.

The X-ray luminosity computed here is the integrated bolometric value, the contribution to either the soft-band or the hard-band individually are likely to be significantly lower. Therefore, we see clearly from Fig. 1, that beyond $z = 1$, we are unlikely to detect any direct X-ray emission from these hot bubbles. However for lower redshift, we see that these sources could have been detected in the current deep X-ray surveys. Therefore, a systematic search for detected extended sources that do not correspond to optically detected clusters in the vicinity of quasars could reveal the presence of these outflows at $z \sim 1$.

Note that we have assumed above that the density contrast between the interior of the bubble and the ambient ISM $\Delta n_e \sim$ an order of magnitude. If indeed the QSO is seeding a proto-cluster, then this contrast can be much larger, implying a much lower density for the ambient medium which in turn (as can be easily seen from eqn (2)) leads to the bubble expanding further out to much larger scales, still getting shock-heated to temperatures of a few times 10^8 K. In this case, the subsequent fragmentation and cooling phases would be delayed. In both scenarios, the optical depth τ has comparable values, $\tau \sim n_e R \sim 10^{-3}$, and therefore, despite their low X-ray luminosity, these hot bubbles are expected to produce thermal Sunyaev-Zeldovich (S-Z) decrements (due to the scattering of the cool microwave background photons off the hot electrons in the bubble) that may be detectable,

$$\frac{\Delta T}{T} = \left(\frac{2kT_e}{m_e c^2} \tau \right) = 3 \times 10^{-5} \left(\frac{T_e}{10^8 \text{ K}} \right). \quad (14)$$

The X-ray emission may only be observable over a small range in redshift, but the temperature decrement may show up at all z as arc-minute scale patches in the cosmic microwave background. A general scenario to explain the detected S-Z decrements (Jones et al. 1996; Richards et al. 1996) in the absence of assembled, hot clusters at high redshift from quasar outflows (both a thermal and a kinematic S-Z component) has been explored by Natarajan & Sigurdsson (1997).

The energy available for the scale of outflows proposed here is more than an order of magnitude lower than for the kinematic case speculated upon by Natarajan & Sigurdsson (1997), with both L_{QSO} and t_Q smaller than envisaged in the relevant section of the earlier paper. In addition to a thermal S-Z decrement

that persists till the gas cools down to $10^6 K$ (akin to the calculation above), they proposed a kinematic S-Z decrement assuming rapid cooling via turbulent mixing. A thermal S-Z effect is temporarily observable while the powering QSO is on, and for a short time afterwards, despite the fact that the gas is unbound, because expansion and hence adiabatic cooling is slow in the self-similar expansion regime. Since it takes the gas, $t \sim R/v_s \sim 3 \times 10^8$ yr (where R is the radius and v_s the sound speed) to cool, the bubble may stay hot for long enough for a detectable thermal S-Z decrement. During the high luminosity phase of the QSO powering the outflow, the S-Z thermal decrement would likely be unobservable because of strong radio lobe emission within the outflow. If the radio lobes fade faster than the gas cools (Rees 1989), then there may be a brief period during which this thermal S-Z effect is observable. In principle, since the frequency dependence of the thermal and kinematic S-Z are different, their relative contributions can be observationally tested.

5. Observational evidence

We now focus on two recent observations that may be consistent with our proposed picture for the modulated galaxy formation around quasars. Pascarelle et al. (1996) reported the discovery of a possible group of sub-galactic clumps at $z = 2.39$ located within an arc-minute of a weak radio galaxy 53W002. Lyman- α emission is detected with equivalent widths of approximately 40 - 50 angstroms, typical of ionization arising purely from young stars, indicative of star-formation activity in these sub-clumps with inferred stellar masses $\leq 10^9 M_\odot$ and star formation rates $\sim 50 M_\odot yr^{-1}$. The magnitudes of these clumps range from M_V of -23 to -18, and if the stellar population is assumed to be young, removing the point source contribution, their inferred luminosities range from (0.1 - 1) L^* . Five of these candidates have confirmed redshifts and three contain weak AGN; the redshift distribution is very narrow $\Delta z \sim 0.01$, consistent with these clumps being distributed in a sheet geometry around the radio galaxy. Additionally, Hu & McMahon (1996) have detected 2 objects during a narrow-band Lyman- α imaging search in a 3.5' X 3.5' region around a $z = 4.55$ quasar. Both objects are at the same redshift as the quasar. They are separated enough spatially (~ 700 kpc) so that the quasar is unlikely to be the source exciting the observed Lyman- α emission, and therefore the emission most probably originates from the star-formation activity within these galaxies.

6. Can we form Globular Clusters?

Here we speculate on the possibility of the formation of globular clusters via the same mechanism, with an attempt to explain the excess number density and possible existence of two distinct populations

of globular cluster systems around some bright elliptical galaxies. From the scaling arguments presented above, we see that weaker outflows (simply scaling down the parameters in this physical picture) might trigger fragmentation to lower mass clumps, which would stall before escaping from the quasar host galaxy. These lower mass clumps should form nearly spherical systems with masses $\sim 10^6 M_\odot$, since the mutual tidal torquing of the clumps cannot impart any significant spin to them.

Observationally, an excess in the number of GCs associated with bright central galaxies is detected (Harris 1996) which fits into this outflow picture. It is possible that a fraction of the population of globular clusters seen around bright cluster galaxies formed in weaker outflows propagating through the IGM, with two-phase warm gas subsequently falling back into the central potential after fragmentation and cooling. The fragments having insufficient velocity to escape the central potential, would stall and collapse in the outskirts of the host galaxy of the quasar, forming a population of nearly co-eval, metal-poor, globular cluster-size stellar clumps. Forming with low angular momentum relative to the centre of the potential, the population would assume an r^{-2} density profile with highly radially anisotropic orbits. Any triaxiality of the central potential would isotropise the spatial distribution of the globular clusters about the galaxy in a few orbital periods, leaving the observed shallow surface density profile of the excess globular population. This scenario therefore predicts that the velocity distribution of the excess globulars ought to be highly radially anisotropic. Recent observational studies of the GC systems around bright ellipticals like M87 (Elson & Santiago 1996), NGC 1399 and N1404 in the Fornax cluster (Forbes et al. 1997) seem to reveal a bimodal colour distribution. In several of these instances, the metal-rich sub-populations are consistent with being more centrally concentrated than the metal-poor ones (NGC 472 - Geisler, Lee & Kim (1996); NGC 5846 - Forbes et al. (1997)). Given these detailed observational studies as well as the theoretical multi-phase collapse model (consisting of 2 episodes of GC formation - one prior to galactic assembly and a second galactic phase) recently proposed by Forbes, Brodie & Grillmair (1997) for the in situ formation of GC systems around ellipticals, our proposed model is appealing since it provides a physical mechanism to form GCs in the pre-galactic phase.

7. Conclusions

We have presented a scenario for the formation of baryon-dominated, low-mass dwarf galaxies at high redshift in the vicinity of quasars. The IGM gas mass swept up by the mechanical luminosity of the outflow from the quasar forms a thin dense shell that expands adiabatically till the age of this gas bubble approaches the Hubble time at the given redshift z , at which juncture the shell fragments due to a Jeans-type gravitational instability producing a characteristic clump mass of $10^9 M_\odot$, leading to the

formation of a group of dwarf galaxies in a sheet-like geometry on roughly an arc-minute scale around the quasar. We predict the properties of this high surface-brightness, low-mass, high redshift dwarf population and demonstrate that the optimal detection strategy would be narrow-band Lyman- α imaging in the regions around high redshift quasars. Examining the feasibility of detection in the X-ray during the early adiabatic expansion phase of the hot bubble, we find that direct X-ray emission is likely to be detectable only from low redshifts ($z < 1$), while measurable thermal S-Z decrements on arc-minute scale patches in the cosmic microwave background are expected from all redshifts. Finally, we argue that a scaled-down version of the same outflow picture could lead to a fragment mass that is typical of GCs, therefore providing a possible physical mechanism for the formation of the older metal-poor, pre-galactic GC population.

Acknowledgments

We thank Martin Rees and Rebecca Elson for many valuable discussions and comments on the manuscript. SS acknowledges the support of the European Union, through a Marie Curie Individual Fellowship. The research of JS has been supported in part by grants from NASA and NSF. JS acknowledges with gratitude the hospitality of the Institut d’Astrophysique de Paris where he is a Blaise-Pascal Visiting Professor, and the Institute of Astronomy at Cambridge, where he has been a Sackler Visiting Astronomer.

REFERENCES

- Babul, A. & Ferguson, H. C., 1996, *ApJ*, 458, 100.
- Babul, A. & Rees, M. J., 1992, *MNRAS*, 255, 346.
- Babul, A. & White, S. D. M., 1991, *MNRAS*, 253, 31.
- Barthel, P. D., & Miley, G. K., 1988, *Nature*, 333, 319.
- Bertschinger, E., 1985, *ApJ*, 295, 1.
- Carr, B., & Ikeuchi, S., 1985, *MNRAS*, 213, 497.
- Ciardullo, R., Jacoby, G., & Ford, H. C., 1989, *ApJ*, 344, 715.
- Ciardullo, R., Jacoby, G., Feldmeier, J., & Bartlett, R., 1997, preprint, astro-ph/9708200.
- Couchman, H. M. P., & Rees, M. J., 1986, *MNRAS*, 221, 53.
- deBlok, W. J. G., McGaugh, S. S., & van der Hulst, J. M., 1996, *MNRAS*, 283, 18.
- Dekel, A., & Silk, J., 1986, *ApJ*, 303, 39.
- Dubinski, J., Mihos, C., & Hernquist, L., 1996, *ApJ*, 462, 576.
- Efstathiou, G., & Rees, M. J., 1988, *MNRAS*, 230, 5.
- Ellis, R. S., 1997, *AR&A*, in press.
- Elson, R. A. W., 1997, *MNRAS*, 286, 771.
- Elson, R. A. W., & Santiago, B. X., 1996, *MNRAS*, 280, 971.
- Ferguson, H. C., Tanvir, N. R., von Hippel, T. et al., 1997, submitted to *Nature*.
- Forbes, D. A., Brodie, J. P., & Grillmair, C. J., 1997, *AJ*, 113, 887.
- Forbes, D. A., Grillmair, C. J., Williger, G. M., Elson, R. A. M., & Brodie, J. P., 1997, preprint, astro-ph/9708025.
- Geisler, D., Lee, M. G., & Kim, E., 1996, *AJ*, 93, 276.
- Harris, W. E., 1991, *Ann. Rev. Astr. Ap.*, 29, 543.
- Heckman, T. M., Armus, L., Miley, G. K., 1987, *AJ*, 93, 276.
- Hu, E., & McMahon, R. G., *Nature*, 382, 231.
- Ikeuchi, S., & Norman, C., 1987, *ApJ*, 312, 485.
- Jones, M., et al., 1996, *ApJ Lett.*, 479, 1.

- Kauffmann, G., White, S. D. M., & Guiderdoni, B., 1993, *MNRAS*, 267, 981.
- Lilly, S. J., Le Fevre, O., Hammer, F., & Crampton, D., 1996, *ApJ Lett.*, 460, 1.
- Madau, P., 1996, preprint, astro-ph/9612157.
- McKee, C., & Ostriker, J. P., 1977, *ApJ*, 218, 148.
- Natarajan, P., & Sigurdsson, S., 1997, preprint, astro-ph/9704237.
- Ostriker, J. P., & Cowie, L., 1981, *ApJ Lett.*, 243, 1270.
- Ostriker, J. P., & Ikeuchi, S., 1983, *ApJ Lett.*, 268, 63.
- Pascarella, S., Windhorst, R., Keel, W., & Odewahn, S., *Nature*, 383, 45.
- Rees, M. J., 1989, *MNRAS*, 239, 1.
- Richards, E. A., Fomalont, E. B., Kellerman, K. I., Partridge, R. B., & Windhorst, R. A., 1997, *AJ*, 113, 1475.
- Steidel, C. S., Adelberger, K. L., Dickinson, M., Giavalisco, M., Pettini, M., & Kellogg, M., 1997, preprint, submitted to *ApJ*, astro-ph/9708125.
- Steidel, C. S., Giavalisco, M., Dickinson, M., & Adelberger, K. L., 1996, *AJ*, 112, 352.
- Tegmark, M., Silk, J., & Evrard, S., 1993, *ApJ*, 417, 54.
- Vishniac, E., Ostriker, J. P., & Bertschinger, E., 1985, *ApJ*, 291, 399.
- Voit, M., 1994, *ApJ Lett.*, 432, 19.
- Voit, M., 1996, *ApJ*, 465, 548.
- White, S. D. M., & Frenk, C. S., 1991, *ApJ*, 379, 52.
- Whitmore, B., Miller, B., Schweizer, F., & Fall, S. M., 1996, *BAAS*, 189, 41-03.

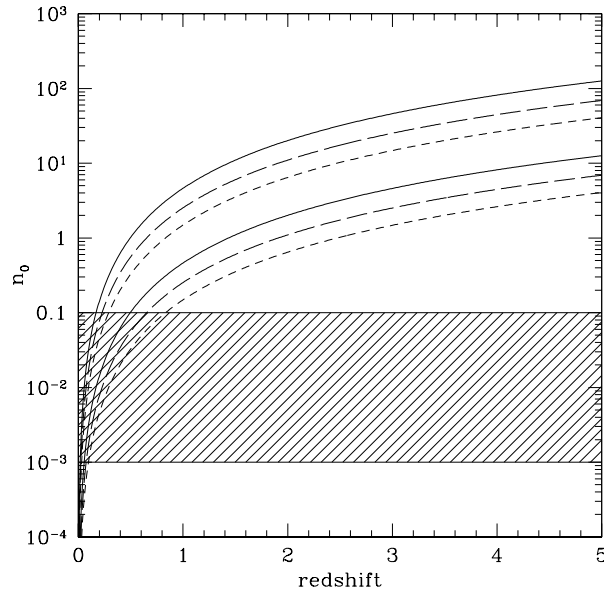


Fig. 1.— The predicted physical properties of the hot gas at the base of the outflow for a 5σ detection at the flux limit of ROSAT (solid curves); ASCA (long-dashed curves) and AXAF (short-dashed curves) following a 10^3 ks integration. The shaded area marks the range in the estimated physical properties of the outflow gas for 2 temperatures 10^8 K (upper curves) and 10^6 K (lower curves).